

Article

Tailored on demand anti-coagulant dosing: an in vitro and in vivo evaluation of 3D printed purpose-designed oral dosage forms

Arafat, Basel, Qinna, Nidal, Cieszyńska, Milena, Forbes, Robert Thomas and Alhnan, Mohamed A

Available at <http://clok.uclan.ac.uk/22564/>

Arafat, Basel, Qinna, Nidal, Cieszyńska, Milena, Forbes, Robert Thomas ORCID: 0000-0003-3521-4386 and Alhnan, Mohamed A (2018) Tailored on demand anti-coagulant dosing: an in vitro and in vivo evaluation of 3D printed purpose-designed oral dosage forms. European Journal of Pharmaceutics and Biopharmaceutics, 128 . pp. 282-289. ISSN 0939-6411

It is advisable to refer to the publisher's version if you intend to cite from the work.
<http://dx.doi.org/10.1016/j.ejpb.2018.04.010>

For more information about UCLan's research in this area go to <http://www.uclan.ac.uk/researchgroups/> and search for <name of research Group>.

For information about Research generally at UCLan please go to <http://www.uclan.ac.uk/research/>

All outputs in CLoK are protected by Intellectual Property Rights law, including Copyright law. Copyright, IPR and Moral Rights for the works on this site are retained by the individual authors and/or other copyright owners. Terms and conditions for use of this material are defined in the [policies](#) page.

1 **Tailored on demand anti-coagulant dosing: an *in vitro* and *in***
2 ***vivo* evaluation of 3D printed purpose-designed oral dosage**
3 **forms**

4
5 Basel Arafat^{1,2}, Nidal Qinna³ Milena Cieszyńska¹, Robert T Forbes¹, Mohamed A
6 Alhnan^{1*}

7
8 ¹ School of Pharmacy and Biomedical Sciences and ² School of Medicine, University of Central
9 Lancashire, Preston, Lancashire, UK.

10 ² Faculty of Medical Sciences and Public health, Anglia Ruskin University, Chelmsford, UK

11 ³ Faculty of Pharmacy and Medical Sciences, University of Petra, Amman, Jordan.

12
13
14
15
16
17 *Corresponding author: MAIbedAlhnan@uclan.ac.uk

ABSTRACT

Coumarin therapy has been associated with high levels of inter- and intra-individual variation in the required dose to reach a therapeutic anticoagulation outcome. Therefore, a dynamic system that is able to achieve accurate delivery of a warfarin dose is of significant importance. Here we assess, the ability of 3D printing to fabricate and deliver tailored individualised precision dosing using an in-vitro model. Sodium warfarin loaded filaments were compounded using hot melt extrusion (HME) and further fabricated *via* fused deposition modelling (FDM) 3D printing to produce capsular-ovoid-shaped dosage forms loaded at 200 and 400 µg dose. The solid dosage forms and comparator warfarin aqueous solutions were administered by oral gavage to Sprague–Dawley rats. *In vitro*, warfarin release was faster at pH 1.2 in comparison to pH 2. A novel UV imaging approach indicated that the erosion of the methacrylate matrix was at a rate of 16.4 and 15.2 µm/min for horizontal and vertical planes respectively. *In vivo*, 3D printed forms were as proportionately effective as their comparative solution form in doubling plasma exposure following a doubling of warfarin dose (184% versus 192% respectively). The 3D printed ovoids showed a lower C_{\max} of warfarin (1.51 and 3.33 mg/mL versus 2.5 and 6.44 mg/mL) and a longer T_{\max} (6 and 3.7 versus 4 and 1.5 h) in comparison to liquid formulation. This work demonstrates for the first time *in vivo*, the potential of FDM 3D printing to produce a tailored specific dosage form and to accurately titrate coumarin dose response to an individual patient.

Keywords: *Rapid prototyping; Patient-centred; Personalized; Patient-specific; Three dimensional printing; additive manufacturing.*

1. Introduction

For over 50 years now, coumarins have been the most prescribed oral anticoagulants.[1] Nevertheless, despite their wide use, coumarin therapy has been associated with a high level of inter-individual variation in dose required to achieve therapeutic anticoagulation response.[2] The administration of an inappropriate warfarin dose for example may place a patient in a hypercoagulable state or increase the patient's risk of bleeding complications early in therapy. As a consequence of over-anticoagulation response, there is an increased risk of major bleeding following the use of anticoagulants by 9.1% [3]. The American College of Chest Physicians (ACCP) supports an “induction” dose of 2 to 5 mg per day which needs to be adjusted according to the patient's International Normalised Ratio (INR)[4]. The pharmacodynamics and pharmacokinetics of coumarins are largely influenced by many factors such as patient age, body weight, dietary vitamin K intake, concomitant medications, as well as various disease states.[2] Hence to ensure that the patient's INR remains within the target range, regular coagulation monitoring and dose modification is necessary.[5]

Nevertheless, limited doses of warfarin tablets are available in the market and dose modification usually requires multiple tablet ingestion or cutting or splitting of larger dose tablets, which could lead to variations in drug content.[6, 7] An area of potential improvement to warfarin therapy would be the ability to produce flexible on-demand precision tailored dose adjustments (particularly given warfarin's due to narrow therapeutic index). One technology that can potentially easily benefit anticoagulant therapy is 3D printing, owing to its flexible and precise manufacturing capability, which enables administration of the lowest effective dose of the drug to maintain the target INR. Indeed, recently, Vuddanda et al. (2017) demonstrated the potential of a re-engineered thermal inkjet printer to address the challenge of warfarin dosage personalisation, achieving highly reproducible minute warfarin dose of approximately 50 µg [8] .

3D printing potential and feasibility has been revealed in several fields such as aerospace, engineering, arts, as well as in fabricating medical implants and devices. Although still at its infancy in the field of personalised medicine, it is expected to revolutionise healthcare and set an innovative platform for pharmaceutical product design and extemporaneous preparation of patient-tailored dosage forms.[9] Fused deposition modelling (FDM) 3D printing, in particular, has been proposed as a platform for controlling the dose.[10] It has demonstrated its capability to manufacture mechanically stable tablets fabricated from pharmaceutical grade polymers without post-processing steps.[10-13] For instance, FDM 3D printing has been viably established using pharmaceutical grade polymers such as PVP [9, 14], methacrylate [15] and cellulose [12] based polymers.

The use of animal models is commonly used to predict formulation behaviour in humans. The use of rats in particular is favoured due to their small size, relatively low cost of breeding and up-keep, as well as the presence of large databases of drug pharmacokinetic data in rats and in humans.[16] Nevertheless, the testing of solid dosage forms in rats presents a challenge in terms of ease of administration. Owing to the need to use a small dosage form size, crushed tablets filled in capsule or suspended in liquid have often been used as an inferior alternative to test the *in vivo* performance of a tablet in rats.[17, 18] However, such approaches significantly alter the nature of the dosage form. More recently, the formulation of mini-tablets for animal use have been attempted [19, 20]. It is therefore important to develop strategies that authentically test intact scaled down human dosage forms for animal studies to enable more reliable extrapolation of human pharmacokinetic responses.

This work aimed to assess the suitability of FDM 3D printer technology for i) fabricating purposely designed solid dosage forms, and ii) tailoring the dose of a narrow therapeutic index drug, namely warfarin. To achieve this goal, rat-tailored FDM 3D printed warfarin ovoid tablets were printed and administered to Sprague–Dawley rats for testing to obtain their pharmacokinetics (PK) parameters.

2. Materials and methods

2.1 Materials

Warfarin (sodium salt) was purchased from Arcos (UK). Eudragit E was donated from Evonik Industries (Darmstadt, Germany). Triethyl citrate (TEC) and tri-calcium phosphate (TCP) were supplied by Sigma–Aldrich (UK). Acetonitrile and methanol were supplied by British Drug Houses (BDH, London, UK). Scotch Blue Painter’s tape 50 mm was supplied by 3M (Bracknell, UK).

2.2 Preparation and optimisation of filaments

In order to fabricate drug-loaded filaments, a hot melt extrusion method was implemented using a Thermo-Scientific HAAKE MiniCTW extruder (Karlsruhe, Germany). A 10 g sample of Eudragit E: TEC: TCP: sodium warfarin 46.75 : 3.25 : 49:1) was accurately weighed and added gradually to counter flow twin-screw hot melt extruder, HAAKE MiniCTW (Karlsruhe, Germany). To allow homogeneous distribution of the powders, the molten mass was mixed in the extruder for at least 5 min prior to extrusion. The specific temperature of initial feeding and extrusion for the filament were 100 and 90 °C respectively. A torque control of 0.8 Nm was used to extrude the filaments. Filaments were stored in sealed plastic bags at room temperature before 3D printing.

2.3 Design and printing of tablets

Tablets were constructed with the pre-prepared filaments using a MakerBot Replicator® 2X Experimental 3D Printer (MakerBot Industries, New York, USA) equipped with 0.4 mm nozzle size. The templates used to print the tablets were designed in a caplet shape using Autodesk® 3ds Max® Design 2016 software version 18.0 (Autodesk, Inc., USA). The design was saved in a stereolithography (.stl) file format and was imported to the 3D printer’s software, MakerWare Version 3.9.1.1143 (Makerbot Industries, LLC., USA).

Two sets of 3D printed tablets were fabricated:

In order to establish the ability of the system to control the low dose of drug for clinical use, a series of tablets with increasing volumes were then printed by increasing the dimensions of the design: length \times width \times heights (L, H, W). The ratios between dimensions ($W = H = 0.4 L$) remained constant. The size of the printed tablet (M) was changed to achieve target doses of 0.5, 1, 3 or 5 mg (Table 1S).

To assess *in vivo* performance of this tablets in rats, a separate set of 3D printed ovoid shapes were manufactured with a cylindrical diameter of 2 mm and lengths of 5.5 or 11 mm to achieve a dose of 200 and 400 μ g respectively. Objects were printed using modified settings of the software as described earlier in our previous work at a temperature of 135 °C. [15]

2.4 Thermal analysis

Samples (raw materials, extruded filaments and printed tablets) were characterised using differential scanning calorimetry (DSC) and thermogravimetric analysis (TGA). For DSC analysis, a differential scanning calorimeter DSC Q2000 (TA Instruments, Elstree, Hertfordshire, UK) with a heating rate of 10 °C/min was used. Samples were heated to 100 °C for 5 min to exclude the effect of humidity then cooled to –20 °C. This was followed by a heat scan from –20 °C to 300 °C. Analysis was carried out under a purge of nitrogen (50 mL/min). The data was analysed using TA 2000 analysis software. Standard 40 µL TA aluminium pans and pin-holed lids were used with an approximate sample mass of 5 mg. All measurements were carried out in triplicate.

For TGA analysis, raw materials, extruded filaments and 3D printed tablets were analysed using a TGA/SDTA851e Mettler Toledo (Leicester, UK). Samples (5 mg, n=3) were placed in 40 µL aluminium pans and were then heated from 25 to 500 °C at a heating rate of 10°C/min and nitrogen gas flow of 50 mL/min. The thermal decomposition (or degradation) profile was analysed using STARE software version 9.00.

2.5 X-ray powder diffraction (XRD)

Samples (raw materials extruded filaments and printed tablets) were characterised using an X-ray diffractometer, D2 Phaser with Lynxeye (Bruker, Germany). Samples were scanned from (2θ)= 5° to 50° using 0.01° step width and a 1 second time count. The divergence slit was 1 mm and the scatter slit 0.6 mm. The wavelength of the X-ray was 0.154 nm using Cu source and a voltage of 30 kV. Filament emission was 10 mA using a scan type coupled with a theta/theta scintillation counter over 60 min.

2.6 Characterisation of tablet properties

The hardness of six ovoid tablets was measured using a TBH 200 (Erweka GmbH, Heusenstamm, Germany). The mean crushing strength was determined, whereby an increasing force was applied to the tablet until it fractured or deformed.

In order to assess the friability of the tablets, 20 tablets were randomly selected, weighed and placed in a friability tester Erweka TAR 10 (Erweka GmbH, Heusenstamm, Germany) and the drum was then rotated at 25 rpm for 4 min. The tablets were reweighed and the differences in weight were calculated and displayed as a percentage of the original sample weight. In order to assess weight uniformity, 10 tablets were randomly selected and weighed. The average weights were measured and the percentage deviation of the individual tablets from the mean was determined.

To assess the impact of both HME and FDM 3D printing on drug content, 3 tablets from each formulation, were randomly selected and weighed. Tablets were then individually placed in a 1000 mL volumetric flask containing 0.1 M HCl and sonicated for 2 h. The solutions were filtered through 0.22 µm Millex-GP syringe filters (Merck Millipore, USA) and prepared for HPLC analysis.

Warfarin concentration in samples was assessed using an Agilent UV-HPLC 1260 series (Agilent Technologies, Inc., Germany) equipped with Kinetex C18 column (100 × 2.1 mm, particle size 2.6 µm) (Phenomenex, Torrance, USA) and set at temperature 26 °C. The mobile phase was 4:1 mixture of methanol: pH 3 water (adjusted with orthophosphoric acid) at a flow rate of 1 mL/min. The injection volume was 100 µL and the stop time was 10 min. The

wavelength was set to 230 nm and the retention time of the drug was 6.3 min with a limit of detection of 0.05 mg/L.

2.7 *In vitro* dissolution studies.

a. Surface dissolution imaging. A Sirius SDi2, the second generation UV imaging system, designed to accommodate whole dosage forms, was used to visualize surface dissolution of sodium warfarin from the 3D printed dosage forms as a whole (Fig. 1). The 3D printed tablets were introduced into the SDi2's flow cell. The dissolution medium (0.1M HCl at 37°C) applied at a flow rate of 8.2 mL/min. The dissolution medium was introduced into the flow cell in the open loop configuration, from bottom to top, with an equivalent linear velocity of 1 cm/min. Dissolution experiments were recorded for a total duration of 60 min. The two dimensional detection area on the SDi2 is significantly larger than for the SDI (24 mm width x 28 mm height) to accommodate dissolution imaging profiling of intact whole dosage forms, with a spatial resolution of 13.75 μ m. The flow cell was illuminated using alternate pulses from two 255 and 520 nm wavelength LEDs. The dual wavelength enables two separate video captures to be produced from a single experiment. Real-time data were then used to measure and differentiate between drug release into solution and tablet erosion from the 255 and 520 nm light obtained videos, respectively.

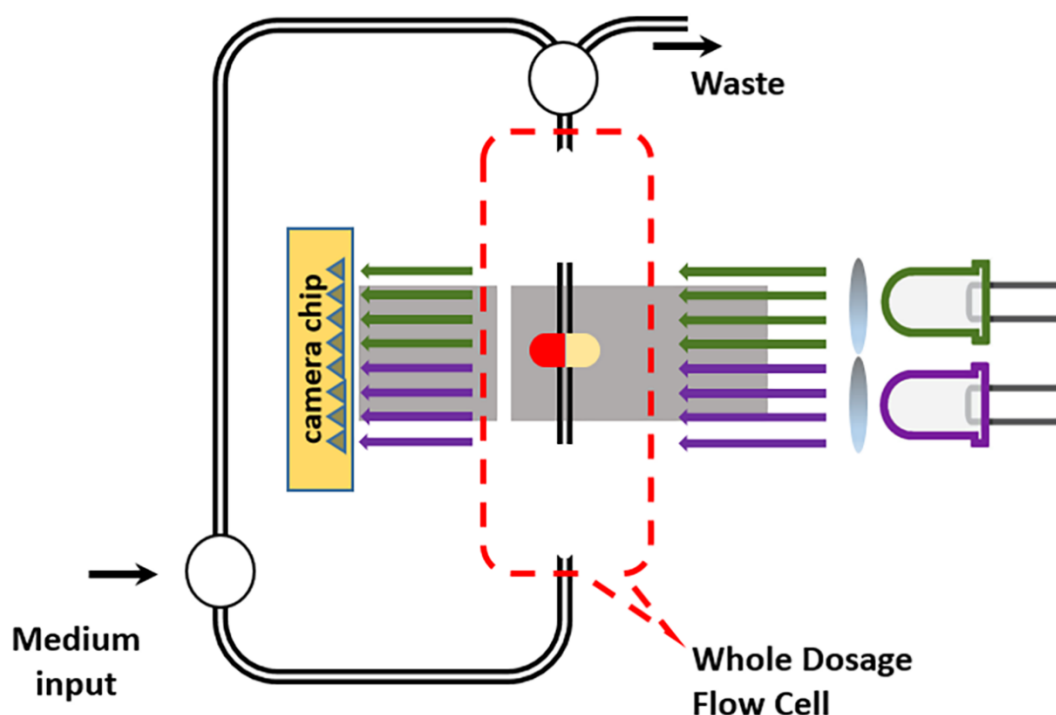


Figure 1. Schematic diagram of SDi2 instrument. LED's of different wavelength are employed to illuminate the 3D printed tablet in flow through cell filled with gastric medium. The obscuration or absorbance of the sample was recorded using an Actipix detector. The medium is pre-heated to 37°C before going through the Whole Dosage Flow Cell and is recirculated in a closed loop configuration.

b. USP II dissolution studies. The *in vitro* release of warfarin from 3D printed tablets was investigated using a USP II Erweka DT600 dissolution tester (Erweka GmbH, Heusenstamm,

Germany). Three tablets were randomly selected and individually placed in the dissolution vessels each containing 900 mL of a fasted state simulated gastric fluid (FaSSGF) (1.75 mM SLS, 0.01N HCl, 0.2% NaCl, pH 2.0) at 50 rpm and 37 ± 0.5 °C. Aliquots (5 mL) were manually collected using 5 mL Leur-Lock syringes at 0, 5, 10, 15, 20, 25, 30, 40, 50 and 60 min time intervals and filtered through an Agilent 0.22 µm filter. Each aliquot withdrawn was replaced with 5 mL of 0.1 M HCl and analysed using the above described HPLC method.

2.8 *In vivo* studies

Adult healthy male Sprague–Dawley rats with an average weight of 240 ± 15 g accommodated at the University of Petra's Animal House (Amman, Jordan) under controlled temperature (22 °C–24 °C), humidity (55%–65%), and a 12 hours photoperiod cycle. All rats were acclimatized for 10 days before experimentation. Rats were weighed and randomized into groups (n=6 rats per cage). Rats were offered standard pellet diet (Jordan Feed Company Ltd., Amman, Jordan) and served clean tap water ad libitum. However, animals were fasted for 18 hours before the day of testing. All experiments were carried out in accordance with University of Petra's Institutional Guidelines on Animal Use that adopts the guidelines of the Federation of European Laboratory Animal Sciences Association (FELASA). The animal study protocols were revised and approved by the Higher Research Council at the Faculty of Pharmacy and Medical Sciences, University of Petra (Amman, Jordan).

3D printed tablets (200 or 400 µg) were administered to the rats *via* any oral capsule stainless steel feeding needle. Comparison control 1 mL warfarin solutions (200 or 400 µg), equivalent to the tablet doses, were freshly prepared and administered to the rats by a stainless steel oral gavage needle (Harvard Apparatus, Kent, UK). Following oral administrations, blood samples were pooled from rat's tail (n=6 rats per group) at different time intervals namely at; 1, 2, 3, 4, 6 and 8 hours post administration. Blood was left to clot, centrifuged for 10 min at 2000G, and then serum was separated and transferred directly into Eppendorf tubes, and kept in a freezer at –20 °C until analysis.

2.9 Analysis of warfarin

For the analysis of warfarin an MS/MS system: API 3200 (Applied Biosystems, MDS SCIEX, USA) attached to Agilent 1200 HPLC (Agilent Technologies, USA) controlled by Analyst 1.6.1 software, was utilised. For the extraction of warfarin from the samples, 100 µL of spiked/blank plasma were pipetted into previously labelled Eppendorf tube, 25 µL of the internal standard (IS) Fenofibric acid (FFA) from 100.0 µg FFA/mL IS solution was added to the tubes and vortexed for 30 sec. Afterwards, the precipitation solution, acetonitrile (400.0 µL) was added to the tube and vortexed for further 1 min. Samples were then centrifuged for 5 min at 14,000 rpm and the supernatant was collated and transferred into an auto-sampler micro vial for analysis. The mobile phase used for analysis comprised of (30:70) mixture of ammonium chloride 0.001M: acetonitrile respectively eluted at a flow rate of 0.7 mL/min through a Thermo BDS Hypersil C18 (50×2.1 mm, particle size 5 µm) column (Thermo Fisher Scientific, Germany) at the temperature 30°C. The injection volume was 5 µL and the stop time was 0.7 min. The retention time of the drug was 0.3 min with a limit of detection of 10 ng/mL.

2.10 Statistical Analysis

Independent sample T-test was also employed using a SPSS Software (22.0.0.2) to analyse the *in vitro* tablet characterisation results. Differences in results where $p \leq 0.05$ were considered significant.

3. Results and discussion

In this study, we explored the adaptability of FDM based 3D printing to engineer and control the dose of immediate release warfarin tablets. When a series of warfarin tablets with increasing dimensions were printed (Fig. 2A, Table S1), a high level of correlation was identified between the theoretical volume of the tablet design and their weights ($R^2=0.9934$) (Fig. 2B). This indicated the ability of FDM 3D printing method to achieve a sufficient control of the mass of 3D printed tablets. To establish the ability of such 3D printing method to control dosage, theoretical doses based on tablet mass and measured dose of warfarin in the tablet were compared. The range of dose accuracy was between 91.5% and 102.4% (Fig. 2C). The coefficient of determination between target and achieved dose ($R^2 = 0.9902$) showed that it is possible to fabricate tablets with desired dose of warfarin through volume modification even at a minute dose of 500 μg (Fig. 2D). With the advances in 3D printers, additional safeguards and quality control mechanisms can be introduced to the evolving technology [21], which are expected to minimise dose variation in the near future.

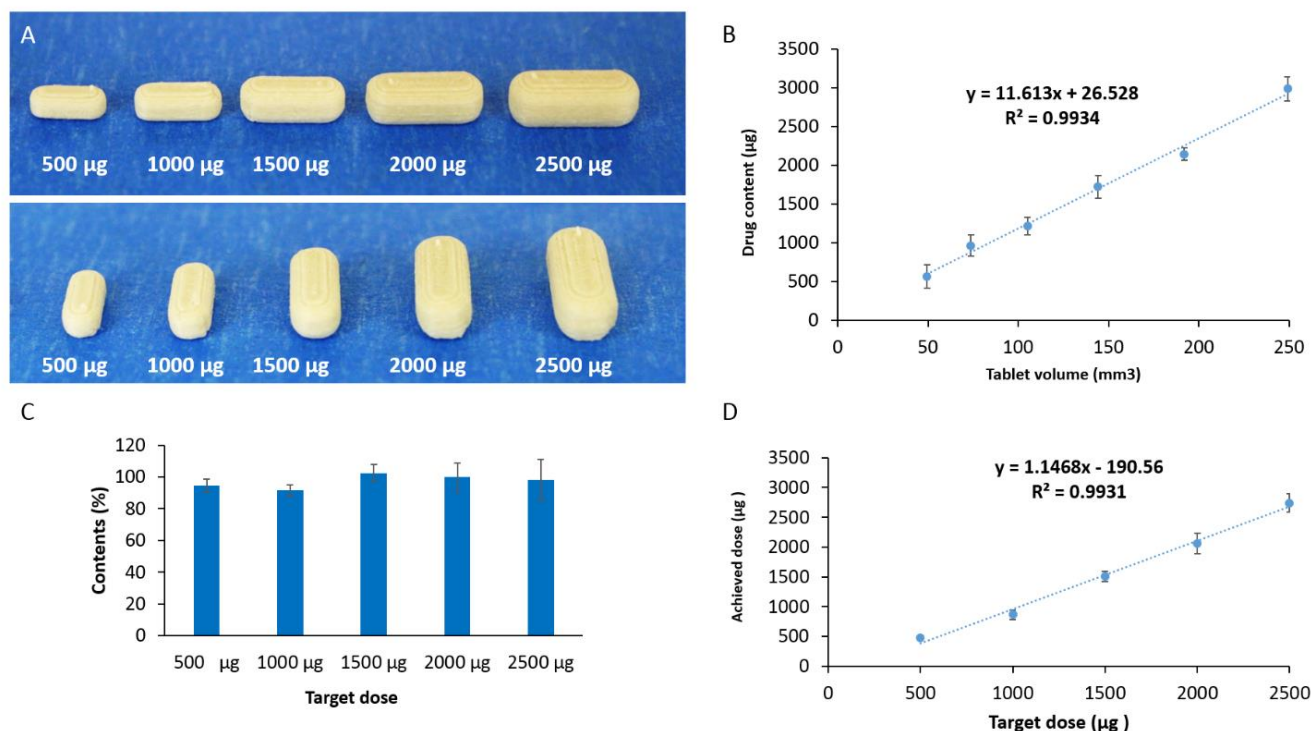


Figure 2. Precision of 3D printing to control low dose sodium warfarin. (A) Images of warfarin loaded FDM 3D printed tablets with increasing dose, (B) Correlation between the theoretical volume and tablet mass, (C) warfarin dose accuracy in the 3D printed tablets and (D) correlation between theoretical volume and warfarin dose ($n=3$, $\pm\text{SD}$).

Profiles from thermogravimetric analyses of warfarin and other additives as well as HME processed filaments and 3D printed tablets are shown in Fig. 3A. Sodium warfarin alone or incorporated in filaments did not suffer a significant weight loss at the printing temperature 135 $^{\circ}\text{C}$. Therefore, it can be assumed that minimal or no degradation of warfarin occurs in the HME as well as in the FDM's nozzle under the utilised temperatures (Fig. 3A). The processing temperatures were lower than the melting point of sodium warfarin (161 $^{\circ}\text{C}$). Differential scanning calorimetry was also conducted to examine the plasticising effect of components on the methacrylic filament. As demonstrated in Fig 3B, the addition of TEC as a plasticizer significantly depressed the T_g of filament to 34 $^{\circ}\text{C}$ from 54 $^{\circ}\text{C}$. However, warfarin was found

to have no significant effect on the Tg of Eudragit E. This could be attributed to the minute percentage of the drug used in the polymeric structure (1% w/w), which was insufficient to significantly influence the mobility of methacrylic polymer chains within the filament matrix. XRD spectra showed that β -calcium tribasic phosphate displayed peaks at 2-theta=17°, 27.8°, 31°, 34.4° corresponding to calcium tribasic phosphate [22], whilst warfarin drug substance showed peaks at 2-theta=12.4° and 18°. XRD spectra of the warfarin filament and tablet showed an absence of these specific peaks [23, 24], suggesting the warfarin is present in an amorphous form within the tablet structure (Fig. 3C).

From determination of the mechanical properties of the 3D printed tablets, the friability of all batches was found to be zero percent. This highlights a prime advantage of FDM 3D printing in generating mechanically stable tablets over its rival technologies such as extrusion 3D printing [25] and powder-based 3D printing. [26, 27] The lack of a drying step or any post-printing finishing procedures, clearly demonstrates the potential of this technology to instantly produce a ready-to-use dosage form within minutes following a healthcare team request.

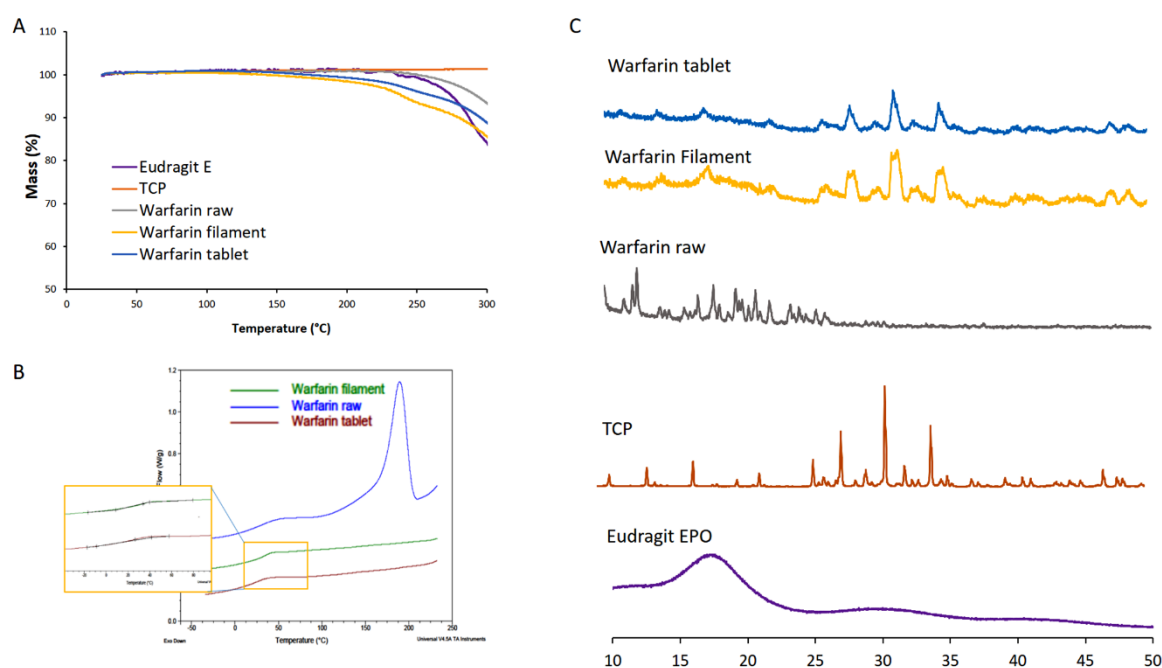


Figure 3. Thermal analysis of Eudragit E based 3D printing filaments. **(A)** Thermal degradation profiles for Eudragit E, sodium warfarin, TCP, warfarin loaded filament and tablet, **(B)** DSC thermograph for warfarin loaded filament and tablet, **(C)** XRD spectra of Eudragit E, TCP, warfarin, and warfarin loaded filament and tablet.

The release pattern of warfarin from the methacrylic matrix was investigated using a modified FaSSGF [28] as a dissolution medium (Fig. 4). All tablets showed a release pattern of > 80% dissolution at 45 min regardless of their individual sizes. The dissolution release profile was attributed to the ionisation of the amino groups of the cationic methacrylic polymer in modified FaSSGF (pH 2.0), which leads to electrostatic repulsion between cationic polymer chains and facilitates polymer dissolution and drug release. The release was compliant with British Pharmacopeia criteria for warfarin tablets [29].

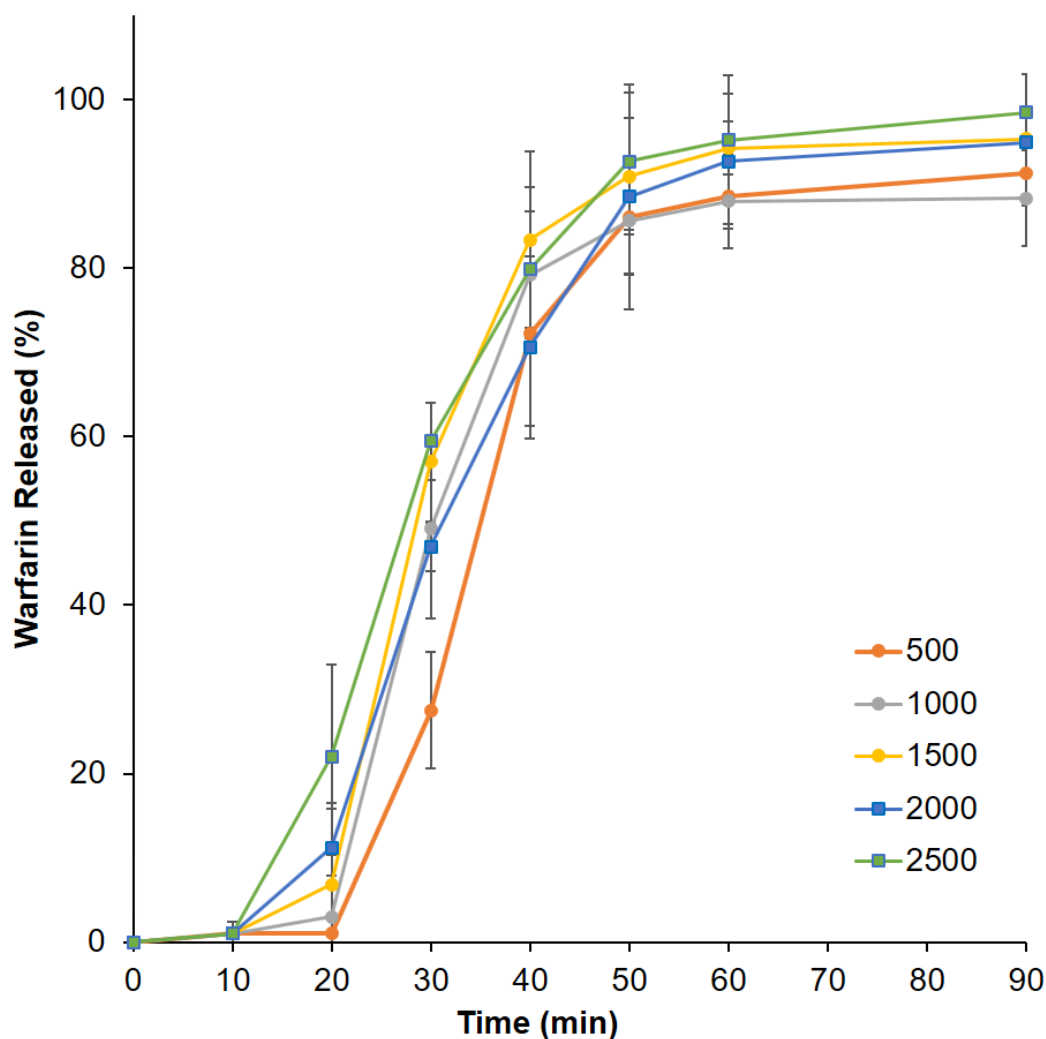


Figure 4. *In vitro* release pattern of sodium warfarin from 3D printed tablets of different doses from a USP II dissolution test in modified FaSSGF (pH 2.0) (n=3, \pm SD).

To better understand the drug release from the 3D printed tablets, the dissolution behaviour of the tablets at the dissolving surface in contact with the dissolution media was explored. A single wavelength system has been previously used to study drug powder dissolution [30]. Here we employ a UV imaging technology capable of generating visual images from simultaneous spectroscopic evaluation for a complete dosage form (Fig. 5A, B). A clear advantage of using such a novel UV-VIS imaging technique over the other well-established imaging techniques lies in the simplicity of operation and interpretation of generated data, analogous to findings by Østergaard.[31] The measurement of light intensity passing through an area of a quartz tube as a function of position and time can also enable quantification of the drug substance at different time intervals. During the dissolution process, drug concentration increased in the first 20 min in the closed loop of the flow-through system. Simultaneously the tablet size was eroded at a rate of 16.4 and 15.2 $\mu\text{m}/\text{min}$ for horizontal and vertical planes respectively. It is worth noting that surface analysis indicated no significant swelling in the first 5 min. The simultaneous drug release data suggested that under the dissolution conditions of study, the majority of drug release took place by a diffusion mechanism before the erosion of the methacrylic matrix within the flow-through cell is complete.

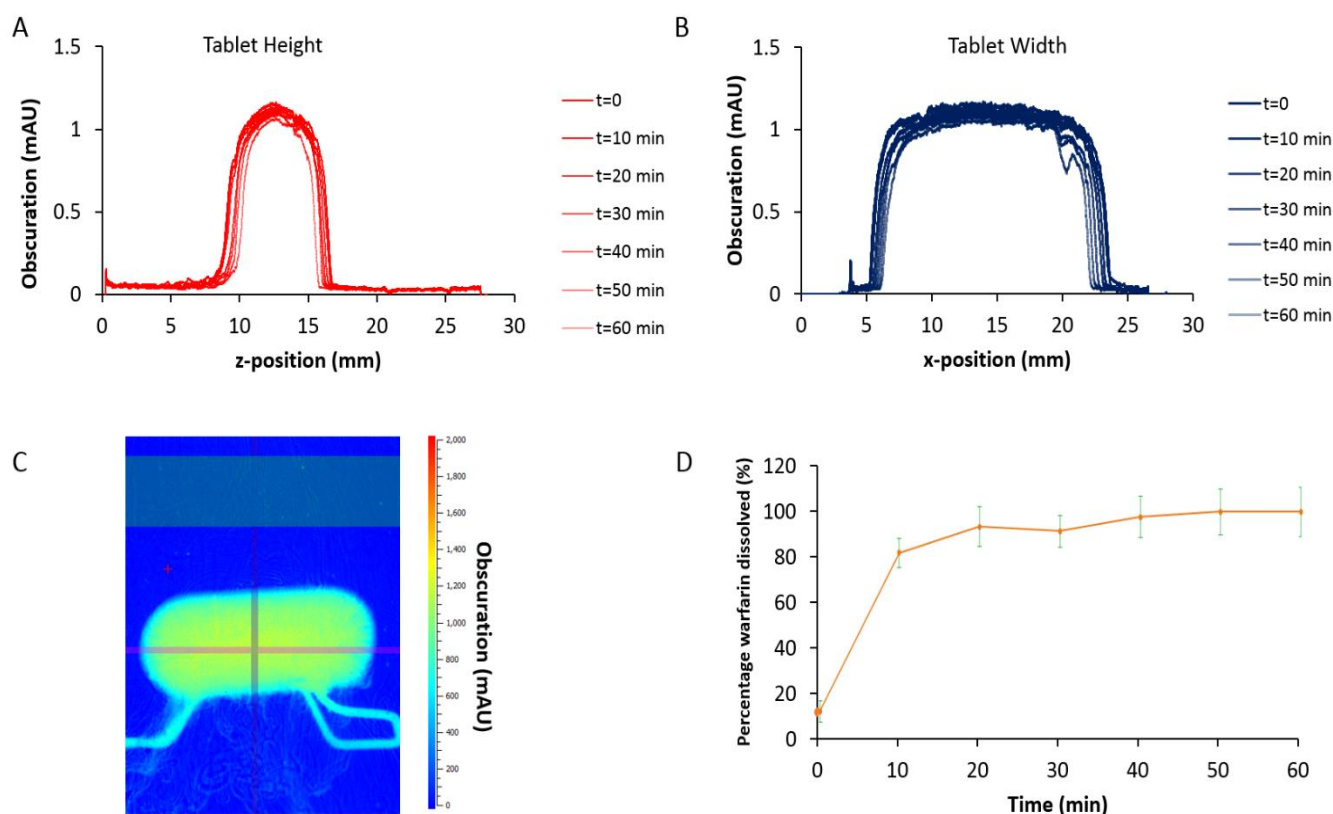


Figure 5. Changes in tablet height (A) and width (B) at 0, 10, 20, 30, 40, 50 and 60 min of the flow through dissolution test using Actipix SDI 2 dissolution imaging technology. (C) UV absorbance image following the illumination of follow cell containing warfarin 3D printed tablet at 255 nm wavelength. (D) Percentage sodium warfarin release from 3D printed tablet during dissolution test (n=3, \pm SD).

A prime advantage of 3D printing technologies lies in their highly flexible nature and capacity to construct dosage forms with accurate spatial distribution of ingredients compared to traditional manufacturing techniques. Therefore, constructs can now be printed to suit the anatomy of not only a particular animal but according to the weight and size of that subject. Rats are commonly considered most suitable for determining the mechanism of drug absorption and bioavailability values from powder or solution formulations [32] as well as micro- or nano-particles [33].

Two different warfarin tablets were specially designed (Fig. 6A1) to mimic the dimensions of commonly used hard capsules intended for oral delivery to rats. Tablets were successfully printed (Fig. 6A2) and were orally gavaged to rats. The pharmacokinetic parameters of warfarin following oral administration either as 3D printed tablets or in a solution form were evaluated (Table 1, Fig. 6B, C). Warfarin plasma exposure was significantly different when an equal dose was administered either as solutions or as 3D printed tablets. The solution showed a markedly higher C_{max} (2.5 and 6.44 mg/mL) and shorter T_{max} (2.67 or 1.5h) for the 200 or 400 μ g/mL solution respectively, in comparison to C_{max} values (1.51 and 3.33 mg/mL) and T_{max} values (6 or 3.7 h) for 200 μ g ($p < 0.05$) and 400 μ g ($p < 0.01$) warfarin tablets respectively.

Table 1. Summary of pharmacokinetic parameters of warfarin following oral gavage of 200 or 400µg from sodium warfarin solution and 3D printed tablets to adult healthy male Sprague–Dawley rats.

Dose	C _{max} * (µg/mL)	T _{max} * (h)	AUC ₁₋₈ * (mg/mL.h)
Solution (200 µg)	2.5±0.3	2.67±1.15	20.64±1.9
Solution (400 µg)	6.44±0.1	1.5±0.6	39.56±7.4
3D printed tablet (200 µg)	1.51±0.09	6±1.6	10.8±2
3D printed tablet (400 µg)	3.33±0.5	3.7±1	19.93±1

* C_{max}, Maximum serum concentration; T_{max}, Time at which C_{max} is observed; and AUC₁₋₈, area under curve.

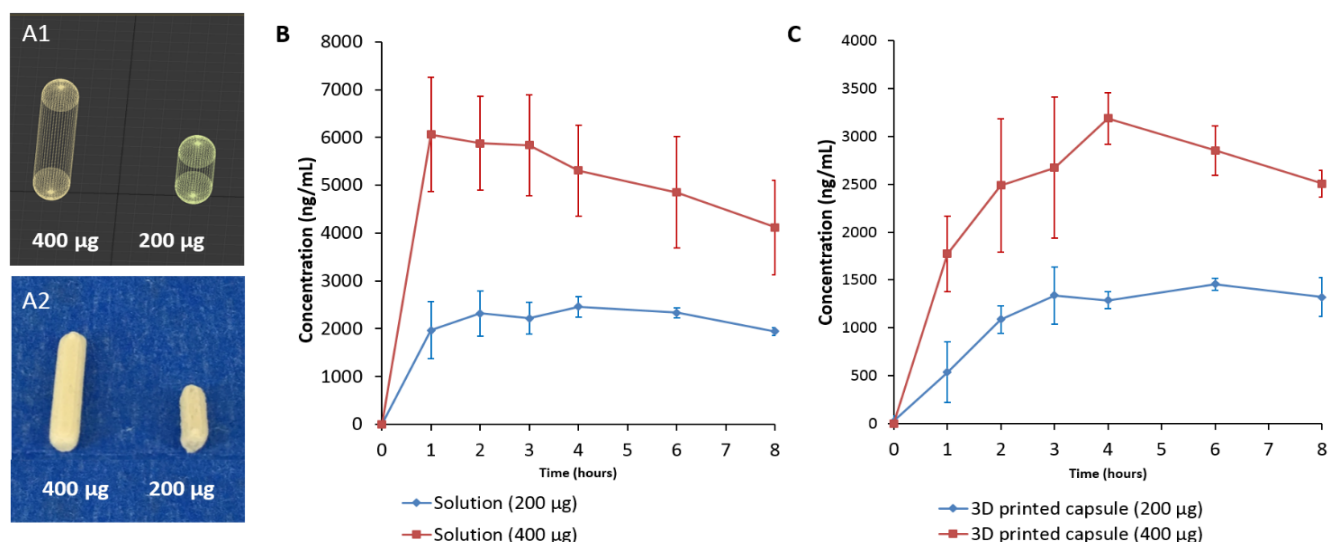


Figure 6. (A1) Rendered images and (A2) photographs of purpose designed 3D printed tablets for oral gavage in rats, (B) Plasma concentration- time profile of warfarin following the oral dosing of 200 or 400µg from (B) warfarin solution and (C) warfarin loaded 3D printed tablets to adult healthy male Sprague–Dawley rats (n=4), error bars ±SD.

Contributing to the finding above, the additional erosion step of Eudragit E in the 3D printed tablets is thought to slow down the release of warfarin from the tablets.. In reality, in an *in vivo* situation, dissolution is expected to be slower than suggested by *in vitro* dissolution techniques since a significantly higher pH of the stomach contents in rats pH 3.2 (fed) and pH 3.9 (fasted) [34] exists compared to the *in vitro* human simulation media conditions. Furthermore, the low fluid volume (3.2±1.8 mL) in the fasted rats are likely to contribute to slower dissolution rates of the methacrylate polymer *in vivo* than *in vitro*. The longer T_{max} of the tablets might also be attributed to the slower transit time of the relatively large oral units in rodents as previously observed to be the case for oral pellets. Such effects are likely to be minimal in healthy human adults where greater volumes of gastric fluids [35, 36] and a lower pH [37] at fasted state are known. In summary, when extrapolating the findings to the human situation, it should be considered that such delay has been augmented by the slower erosion of cationic polymer in rat gastric environments rats due to their relatively higher gastric pH and lower fluid contents in comparison to humans. A key driver in the uptake and use of these polymer-rich tablets

(yielded by FDM 3D printing) is that they match the release from standard compressed powdered tablets. The data we present suggests that dissolution of 3D tablets requires acceleration. However recently, there has been reports of utilizing 3D printer geometry to fabricate tablet with complex structure to accelerate drug release [38, 39].

On the other hand, 3D printed tablets were proportionately effective as solution formulations, in that a doubling of warfarin dose from the either tablet or solution resulted in a rough doubling of measured plasma exposure with AUC₁₋₈ values doubling from 20.64±1.9 to 39.56±7.4 µg/mL for the 200 and 400 µg/mL solutions respectively and from 10.8±2 to 19.93±1 µg/mL for the 200 and 400 µg 3D printed capsules, respectively (184 % versus 192% respectively). Envisioning a future scenario, a healthcare staff member may be able to use computer software to digitally directly tailor and manufacture an individualised precision dose and consequently provide plasma levels of warfarin appropriate to an individual patient's need.

In summary, the findings in this study clearly demonstrate the potential of 3D printing as a platform to design animal-suitable solid dosage forms and thus in principle provide a pathway for human use with the potential advantage of digitally titrating an individuals dose in response to clinical data. We have also shown the utility of a novel dissolution imaging system to give mechanistic insights into the dissolution process of a 3D-printed tablet dosage form.

4. Conclusions

This study demonstrates the flexibility of FDM 3D printers to fabricate solid dosage forms to purposely suit the anatomy of an animal subject. UV imaging indicated that the erosion of methacrylic matrix takes place at 16.4 and 15.2 $\mu\text{m}/\text{min}$ for horizontal and vertical planes respectively and resulted in delayed plasma exposure in comparison to warfarin solutions. Moreover, the titration of dose of a narrow therapeutic index drug, warfarin, has been demonstrated *in vitro* and *in vivo*. In principle, the technology holds the promise to provide a much more dynamic and responsive anticoagulant regime to suit a constantly changing patient's INR profile. Such an approach can provide patients with a safer, more accurate and computerised alternative to the more commonly used approach of dosing using multiple tablets to include tablet splitting.

Acknowledgments

The authors would like to thank UCLAN Innovation Team for this support and Mrs Reem Arafat for her help with graphics design.

Conflicts of interest M A Alhnan is the innovator in patent applications WO 2016038356 A1, WO2017072536A1 and WO2018020237A1 in the field of 3D printing of medicines.

397 **References**

- 398 [1] K.A. Bauer, Pros and cons of new oral anticoagulants, ASH Education Program Book, 2013
399 (2013) 464-470.
- 400 [2] H. Takahashi, H. Echizen, Pharmacogenetics of CYP2C9 and interindividual variability in
401 anticoagulant response to warfarin, *Pharmacogenomics J*, 3 (2003) 202-214.
- 402 [3] L.A. Linkins, P.T. Choi, J.D. Douketis, Clinical impact of bleeding in patients taking oral
403 anticoagulant therapy for venous thromboembolism: a meta-analysis, *Ann Intern Med*, 139
404 (2003) 893-900.
- 405 [4] J. Hirsh, J. Dalen, D.R. Anderson, L. Poller, H. Bussey, J. Ansell, D. Deykin, Oral
406 anticoagulants: mechanism of action, clinical effectiveness, and optimal therapeutic range,
407 *Chest*, 119 (2001) 8S-21S.
- 408 [5] M. Kuruvilla, C. Gurk-Turner, A review of warfarin dosing and monitoring, *Proceedings*
409 (Baylor University. Medical Center), 14 (2001) 305-306.
- 410 [6] S.W. Hill, A.S. Varker, K. Karlage, P.B. Myrdal, Analysis of drug content and weight
411 uniformity for half-tablets of 6 commonly split medications, *J Manag Care Pharm*, 15 (2009)
412 253-261.
- 413 [7] J.E. Polli, S. Kim, B.R. Martin, Weight uniformity of split tablets required by a Veterans
414 Affairs policy, *J Manag Care Pharm*, 9 (2003) 401-407.
- 415 [8] P.R. Vuddanda, M. Alomari, C.C. Dadoo, S.J. Trenfield, S. Velaga, A.W. Basit, S. Gaisford,
416 Personalisation of warfarin therapy using thermal ink-jet printing, *Eur J Pharm Sci*, 117 (2018)
417 80-87.
- 418 [9] T.C. Okwuosa, D. Stefaniak, B. Arafat, A. Isreb, K.W. Wan, M.A. Alhnan, A Lower
419 Temperature FDM 3D Printing for the Manufacture of Patient-Specific Immediate Release
420 Tablets, *Pharm Res*, 33 (2016) 2704-2712.
- 421 [10] J. Skowrya, K. Pietrzak, M.A. Alhnan, Fabrication of extended-release patient-tailored
422 prednisolone tablets via fused deposition modelling (FDM) 3D printing, *Eur J Pharm Sci*, 68
423 (2015) 11-17.
- 424 [11] A. Goyanes, P. Robles Martinez, A. Buanz, A.W. Basit, S. Gaisford, Effect of geometry on
425 drug release from 3D printed tablets, *Int J Pharm*, 494 (2015) 657-663.
- 426 [12] K. Pietrzak, A. Isreb, M.A. Alhnan, A flexible-dose dispenser for immediate and extended
427 release 3D printed tablets, *Eur J Pharm Biopharm*, 96 (2015) 380-387.
- 428 [13] A. Goyanes, H. Chang, D. Sedough, G.B. Hatton, J. Wang, A. Buanz, S. Gaisford, A.W. Basit,
429 Fabrication of controlled-release budesonide tablets via desktop (FDM) 3D printing, *Int J*
430 *Pharm*, 496 (2015) 414-420.
- 431 [14] T.C. Okwuosa, B.C. Pereira, B. Arafat, M. Cieszyńska, A. Isreb, M.A. Alhnan, Fabricating a
432 Shell-Core Delayed Release Tablet Using Dual FDM 3D Printing for Patient-Centred Therapy,
433 *Pharm Res*, 34 (2017) 427-437.
- 434 [15] M. Sadia, A. Sosnicka, B. Arafat, A. Isreb, W. Ahmed, A. Kelarakis, M.A. Alhnan, Adaptation
435 of pharmaceutical excipients to FDM 3D printing for the fabrication of patient-tailored
436 immediate release tablets, *Int J Pharm*, 513 (2016) 659-668.
- 437 [16] X. Cao, S.T. Gibbs, L. Fang, H.A. Miller, C.P. Landowski, H.C. Shin, H. Lennernas, Y. Zhong,
438 G.L. Amidon, L.X. Yu, D. Sun, Why is it challenging to predict intestinal drug absorption and
439 oral bioavailability in human using rat model, *Pharm Res*, 23 (2006) 1675-1686.
- 440 [17] D. Mann, US Patent 4637816 A: Apparatus for the oral administration of capsules to
441 animals, in, 1987.

442 [18] Z. Atcha, C. Rourke, A.H. Neo, C.W. Goh, J.S. Lim, C.C. Aw, E.R. Browne, D.J. Pemberton,
 443 Alternative method of oral dosing for rats, *J Am Assoc Lab Anim Sci*, 49 (2010) 335-343.

444 [19] A. Vetter, G. Perera, K. Leithner, G. Klima, A. Bernkop-Schnurch, Development and in vivo
 445 bioavailability study of an oral fondaparinux delivery system, *Eur J Pharm Sci*, 41 (2010) 489-
 446 497.

447 [20] J.Y. Kim, H.J. Bae, J. Choi, J.R. Lim, S.W. Kim, S.H. Lee, E.S. Park, Efficacy of gastro-retentive
 448 forms of ecabet sodium in the treatment of gastric ulcer in rats, *Arch Pharm Res*, 37 (2014)
 449 1053-1062.

450 [21] N. Sandler, I. Kassamakov, H. Ehlers, N. Genina, T. Ylitalo, E. Haeggstrom, Rapid
 451 interferometric imaging of printed drug laden multilayer structures, *Sci Rep*, 4 (2014) 4020.

452 [22] Brian R. Genge, Licia Wu, Glenn R. Sauer, Roy E. Wuthier, R. Genge, US Patent 7527687
 453 B2 Biocompatible cement containing reactive calcium phosphate nanoparticles and methods
 454 for making and using such cement., in, 2009.

455 [23] A. Nguyenpho, A.B. Ciavarella, A. Siddiqui, Z. Rahman, S. Akhtar, R. Hunt, M. Korang-
 456 Yeboah, M.A. Khan, Evaluation of In-Use Stability of Anticoagulant Drug Products: Warfarin
 457 Sodium, *J Pharm Sci*, 104 (2015) 4232-4240.

458 [24] Z. Rahman, M. Korang-Yeboah, A. Siddiqui, A. Mohammad, M.A. Khan, Understanding
 459 effect of formulation and manufacturing variables on the critical quality attributes of warfarin
 460 sodium product, *Int J Pharm*, 495 (2015) 19-30.

461 [25] S.A. Khaled, J.C. Burley, M.R. Alexander, C.J. Roberts, Desktop 3D printing of controlled
 462 release pharmaceutical bilayer tablets, *Int J Pharm*, 461 (2014) 105-111.

463 [26] D.-G. Yu, C. Branford-White, Y.-C. Yang, L.-M. Zhu, E.W. Welbeck, X.-L. Yang, A novel fast
 464 disintegrating tablet fabricated by three-dimensional printing, *Drug Dev Ind Pharm*, 35 (2009)
 465 1530-1536.

466 [27] W.E. Katstra, R.D. Palazzolo, C.W. Rowe, B. Giritlioglu, P. Teung, M.J. Cima, Oral dosage
 467 forms fabricated by Three Dimensional Printing™, *J Control Release*, 66 (2000) 1-9.

468 [28] A. Aburub, D.S. Risley, D. Mishra, A critical evaluation of fasted state simulating gastric
 469 fluid (FaSSGF) that contains sodium lauryl sulfate and proposal of a modified recipe, *Int J*
 470 *Pharm*, 347 (2008) 16-22.

471 [29] B. comission, British Pharmacopeia 2017, The British Pharmacopoeia Commission (BCP)
 472 Office, London, 2017.

473 [30] W.L. Hulse, J. Gray, R.T. Forbes, A discriminatory intrinsic dissolution study using UV area
 474 imaging analysis to gain additional insights into the dissolution behaviour of active
 475 pharmaceutical ingredients, *Int J Pharm*, 434 (2012) 133-139.

476 [31] J. Ostergaard, UV imaging in pharmaceutical analysis, *J Pharm Biomed Anal*, (2017).

477 [32] T.T. Kararli, Comparison of the Gastrointestinal Anatomy, Physiology, and Biochemistry
 478 of Humans and Commonly Used Laboratory-Animals, *Biopharmaceutics & Drug Disposition*,
 479 16 (1995) 351-380.

480 [33] M. Mori, Y. Shirai, Y. Uezono, T. Takahashi, Y. Nakamura, H. Makita, Y. Nakanishi, Y.
 481 Imasato, Influence of specific gravity and food on movement of granules in the
 482 gastrointestinal tract of rats, *Chem Pharm Bull (Tokyo)*, 37 (1989) 738-741.

483 [34] E.L. McConnell, A.W. Basit, S. Murdan, Measurements of rat and mouse gastrointestinal
 484 pH, fluid and lymphoid tissue, and implications for in-vivo experiments, *J Pharm Pharmacol*,
 485 60 (2008) 63-70.

[35] F. Gotch, J. Nadell, I.S. Edelman, Gastrointestinal water and electrolytes. IV. The equilibration of deuterium oxide (D₂O) in gastrointestinal contents and the proportion of total body water (T.B.W.) in the gastrointestinal tract, *J Clin Invest*, 36 (1957) 289-296.

[36] C. Tuleu, C. Andrieux, P. Boy, J.C. Chaumeil, Gastrointestinal transit of pellets in rats: effect of size and density, *Int J Pharm*, 180 (1999) 123-131.

[37] D.F. Evans, G. Pye, R. Bramley, A.G. Clark, T.J. Dyson, J.D. Hardcastle, Measurement of gastrointestinal pH profiles in normal ambulant human subjects, *Gut*, 29 (1988) 1035-1041.

[38] M. Kyobula, A. Adedeji, M.R. Alexander, E. Saleh, R. Wildman, I. Ashcroft, P.R. Gellert, C.J. Roberts, 3D inkjet printing of tablets exploiting bespoke complex geometries for controlled and tuneable drug release, *J Control Release*, 261 (2017) 207-215.

[39] M. Sadia, B. Arafat, W. Ahmed, R.T. Forbes, M.A. Alhnan, Channelled tablets: An innovative approach to accelerating drug release from 3D printed tablets, *J Control Release*, 269 (2018) 355-363.

List of Figures

Figure 1. Schematic diagram of SDi2 instrument. LED's of different wavelength are employed to illuminate the 3D printed tablet in flow through cell filled with gastric medium. The obscuration or absorbance of the sample was recorded using an Actipix detector. The medium is pre-heated to 37°C before going through the Whole Dosage Flow Cell and is recirculated in a closed loop configuration.

Figure 2. Precision of 3D printing to control low dose sodium warfarin. (A) Images of warfarin loaded FDM 3D printed tablets with increasing dose, (B) Correlation between the theoretical volume and tablet mass, (C) warfarin dose accuracy in the 3D printed tablets and (D) correlation between theoretical volume and warfarin dose (n=3, ±SD).

Figure 3. Thermal analysis of Eudragit E based 3D printing filaments. (A) Thermal degradation profiles for Eudragit E, sodium warfarin, TCP, warfarin loaded filament and tablet, (B) DSC thermograph for warfarin loaded filament and tablet, (C) XRD spectra of Eudragit E, TCP, warfarin, and warfarin loaded filament and tablet.

Figure 4. *In vitro* release pattern of sodium warfarin from 3D printed tablets of different doses from a USP II dissolution test in modified FaSSGF (pH 2.0) (n=3, ±SD).

Figure 5. Changes in tablet height (A) and width (B) at 0, 10, 20, 30, 40, 50 and 60 min of the flow through dissolution test using Actipix SDI 2 dissolution imaging technology. (C) UV absorbance image following the illumination of flow cell containing warfarin 3D printed tablet at 255 nm wavelength. (D) Percentage sodium warfarin release from 3D printed tablet during dissolution test (n=3, ±SD).

Figure 6. (A1) Rendered images and (A2) photographs of purpose designed 3D printed tablets for oral gavage in rats, (B) Plasma concentration- time profile of warfarin following the oral dosing of 200 or 400µg from (B) warfarin solution and (C) warfarin loaded 3D printed tablets to adult healthy male Sprague–Dawley rats (n=4), error bars ±SD.

List of tables

Table 1. Summary of pharmacokinetic parameters of warfarin following oral gavage of 200 or 400µg from sodium warfarin solution and 3D printed tablets to adult healthy male Sprague–Dawley rats.

Supplementary data

527 **Table 1S.** Summary of length, width, height and volume of cuboid containing warfarin loaded 3D
528 printed tablets.

529

Tailored on demand anti-coagulant dosing: an *in vitro* and *in vivo* evaluation of 3D printed purpose-designed oral dosage forms

Basel Arafat^{1,2}, Nidal Qinna² Milena Cieszynska¹, Robert T Forbes¹, Mohamed A Alhnan^{1*}

¹School of Pharmacy and Biomedical Sciences and ²School of Medicine, University of Central Lancashire, Preston, Lancashire, UK.

² Faculty of Pharmacy and Medical Sciences, University of Petra, Amman, Jordan.

Supplementary Data

*Corresponding author: MAIbedAlhnan@uclan.ac.uk

Table 1S. Summary of length, width, height and volume of cuboid containing sodium warfarin loaded 3D printed tablets

Target dose (µg)	Volume (mm³)	X (mm)	Y (mm)	Z (mm)
300	19.06	5.09	1.86	2.00
500	40.74	6.55	2.40	2.58
1000	94.93	8.68	3.18	3.42
1500	149.12	10.09	3.69	3.98
2000	203.31	11.19	4.09	4.41
2500	257.51	12.10	4.43	4.77
3000	311.70	12.90	4.72	5.08
4000	420.08	14.24	5.21	5.61
5000	528.47	15.38	5.62	6.06